Terminally differentiated astrocytes lack DNA damage response signaling and are radioresistant but retain DNA repair proficiency

Leonid Schneider, Marzia Fumagalli, Fabrizio d'Adda Di Fagagna

Terminally differentiated astrocytes lack DNA damage response signaling and are radioresistant but retain DNA repair proficiency

Running title:

DNA damage response signaling is functional in neural stem cells and absent in terminally differentiated astrocytes

Leonid Schneider[1], Marzia Fumagalli[1] and Fabrizio d'Adda di Fagagna[1]

[1] *IFOM Foundation - The FIRC Institute of Molecular Oncology Foundation, Via Adamello 16, 20139 Milan, Italy*

Corresponding authors: Fabrizio d'Adda di Fagagna, Leonid Schneider

tel. +39 02 574303.227, fax +39 02 574303.231

email: fabrizio.dadda@ifom-ieo-campus.it, leonid.schneider@ifom-ieo-campus.it

Abstract

The impact and consequences of damage generation into genomic DNA, especially in the form of DNA double-strand breaks (DSB), and of the DNA damage response (DDR) pathways that are promptly activated have been elucidated in great detail [1-2]. Most of this research, however, has been performed on proliferating, often cancerous, cell lines. In a mammalian body, the majority of cells is terminally differentiated (TD), and derives from a small pool of self-renewing somatic stem cells.

Here, we comparatively studied DDR signaling and radiosensitivity in neural stem cells (NSC) and their TD-descendants, astrocytes – the predominant cells in the mammalian brain. Astrocytes play important roles in brain physiology, development and plasticity [3]. We discovered that NSC activate canonical DDR upon exposure to ionizing radiation. Strikingly, astrocytes proved radioresistant, lacked functional DDR signaling, with key DDR genes such as ATM being repressed at the transcriptional level. Nevertheless, astrocytes retain the expression of non-homologous end joining (NHEJ) genes and indeed they are DNA repair proficient. Unlike in NSC, in astrocytes DNA-PK seems to be the PI3K-like protein kinase responsible for γH2AX signal generation upon DNA damage. We also demonstrate the lack of functional DDR signaling activation *in vivo* in astrocytes of irradiated adult mouse brains, while adjacent neurons activate the DDR.

Keywords

DNA Damage Response, Astrocytes, Neural Stem Cells

Introduction

Damage to genomic DNA elicits swift activation of DNA damage response (DDR), a molecular signaling cascade, which coordinates DNA repair, cell cycle arrest, and ultimately apoptosis or cellular senescence. Presently, most of DDR research is performed on proliferating and often transformed cells or, occasionally, transiently-arrested quiescent cells. Yet the overwhelming majority of cells in multicellular organisms is terminally differentiated (TD) and does not proliferate. Non-dividing TD cells of the soma derive from proliferating or proliferation-proficient somatic stem and progenitor cells. However, it is unclear whether, and to which extent, somatic stem cells and their TD descendants respond to DNA damage by engaging the canonical DDR pathways observed in most commonly experimentally used cell systems. Likewise, the radiosensitivity of these two distinct cell types is poorly characterized.

The canonical DDR pathways are now well elucidated [1-2]. DNA double strand breaks (DSB) generation triggers the autophosphorylation and consequent activation of the apical PI3K-like protein kinase ATM at Serine 1981 (S1981), which is detectable in the form of nuclear foci assembling at DSB sites [4]. Upon activation, ATM labels chromatin break sites over large distances of the chromosome through Serine139 (S139) phosphorylation of the histone H2A variant H2AX (γH2AX) [5]. The serine/threonine kinase ATM targets a large number of downstream effectors with various enzymatic and transcriptional regulation capacities by phosphorylating their evolutionarily conserved serine/threonine-glutamine (S/TQ) target motif [1]. Some of these effectors, such as 53BP1 are focally recruited by ATM to DSB [6-7]. Protein kinases like CHK2 and transcription

factors like p53 further relay DDR signaling throughout the nucleus ultimately regulating cell cycle progression and survival [1-2].

DSB can be repaired by two major mechanisms. Homologous recombination (HR) operates mainly in S-G2 phases [8], therefore it is not active in G_0-arrested and terminally differentiated cells. In these cells, DSB repair relies mainly on non-homologous end-joining (NHEJ) [8]. This pathway depends on the activity of a PI3K-like DNA-dependent protein kinase (DNA-PK), which consists of DNA-PK catalytic subunit (DNA-PKcs), KU70 and KU80 subunits of the KU heterodimer, and on the activity of DNA ligase IV and its associated cofactor XRCC4 [9]. Similarly to ATM, DNA-PK preferentially recognizes and phosphorylates a S/TQ motif [9].

In this study we addressed DDR signaling and radioresistance of TD astrocytes, which are the predominant cell type in the mammalian brain and play key roles in brain physiology, development and plasticity [3]. Glial cells like astrocytes, but also neurons, derive from neural stem cells (NSC) residing in specific brain areas [10]. It is known from previous studies that ionizing radiation received prenatally from atom bomb explosions in Japan have debilitating effects on human brain development [11] and the risk of mental retardation is a crucial safety issue for radiation therapy during pregnancy [12]. We see it necessary to combine today's knowledge of stem cells, differentiation and molecular DDR signaling to better understand the impact of DNA damage generation in the brain. In our study, we interrogate murine NSC and their TD descendants astrocytes by comparatively testing the functionality of their DDR pathways at the molecular level *in vitro* and *in vivo*.

Results

In order to comparatively assess DDR signaling in somatic stem cells and their TD descendants, we employed murine ES-cell derived NSC, which are fully tri-potent in their ability to differentiate into neurons, oligodendrocytes and astrocytes [13]. We employed the established method of rapid and efficient differentiation of NSC into astrocytes by supplementing growth medium with fetal calf serum (FCS) [13]. FCS induces a proliferative arrest associated with morphological changes typical of astrocytic differentiation in all cultured cells within 24-48 hours (Fig. S1 and data not shown); in order to assure a complete terminal differentiation, all experiments were performed 7 days following FCS treatment.

First, we aimed to determine whether NSC and NSC-derived astrocytes exposed to X-rays are capable of responding to genotoxic insults by the activation of a robust canonical DDR. For this purpose, we studied the formation of nuclear foci of the activated key components of the DDR signaling cascade by means of immunofluorescence analysis and confocal microscopy. In order to ascertain the differential cell types studied, we took advantage of the fact that NSC are virtually negative for the intermediate filament glial fibrillary acidic protein (GFAP), while TD-astrocytes express high levels of GFAP ([13] and Fig. 1). As readout for DDR activation, we stained NSC and astrocytes for the auto-phosphorylated and thus activated form of ATM (ATM-pS1981), for phosphorylated S/TQ epitope (pS/TQ), 53BP1 and γH2AX foci one hour after exposure of cells to X-rays (10Gy). We observed that NSC show bright nuclear foci for all the four markers analyzed, while not irradiated cells showed virtually no nuclear foci assembly (Fig. 1A

and Fig. S2). Astrocytes however, when processed in parallel, show a comparably strongly reduced phospho-ATM foci formation and no detectable pS/TQ or 53BP1 nuclear foci one hour after irradiation. Even a large dose of 50Gy fails to elicit 53BP1 foci formation in astrocytes (Fig. S3). Remarkably though, γH2AX is still clearly detectable in astrocytes, indicating the presence of irradiation-induced S/TQ kinase activity (Fig. 1B and Fig. S2). In order to ascertain the co-localisation of γH2AX foci with other DDR markers, such as 53BP1, we irradiated NSC and astrocytes with 1Gy only (Fig. S3). Due to fewer DSB generated, discrete and separate γH2AX foci can be clearly detected in NSC and astrocytes and, in the former, γH2AX and 53BP1foci neatly co-localize.

Next we investigated whether the suppressed DDR signaling in astrocytes might be the consequence of altered expression pattern of DDR gene associated with astrocytic differentiation. We comparatively quantified the mRNA expression levels of DDR factors ATM, MRE11, MDC1, CHK2 and p53 by quantitative RT-PCR (qRT-PCR) in TD-astrocytes versus NSC. We found all these genes to be transcriptionally strongly downregulated in astrocytes when considering their individual expression levels in NSC as reference (Fig. 2A). While DDR signaling was suppressed, our qRT-PCR analysis however revealed that the non-homologous end-joining (NHEJ) pathway of DNA repair was not significantly downregulated (Fig. 2A), as shown for DNA-PKcs, KU70, KU80, Ligase 4 (LIG4), XRCC4, and 53BP1 gene expression levels – the latter was recently reported to be involved also in DNA repair [14].

We then comparatively studied the ATM-dependent DDR signaling in irradiated NSC and astrocytes by the means of western blot analyses. In NSC, irradiation lead to ATM

autophosphorylation and a mobility shift of CHK2, suggesting its DNA damage-induced phosphorylation, while in astrocytes phospho-ATM was not detectable at 1h or 24h after irradiation and CHK2 protein was completely absent (Fig. 2B), in agreement with their gene expression profiles (Fig. 2A). Reflecting the insufficient ATM signaling in astrocytes, 53BP1 was not recruited or retained at the DNA damage sites (Fig. 1B), despite being expressed in astrocytes at levels comparable to NSC (Fig. 2A,B).

We also determined that DNA damage-induced phosphorylation of p53 at Serine-15 (S15, a residue targeted by ATM) and accumulation of p53 protein [15], were fully functional in NSC, while less pronounced in irradiated astrocytes (Fig. 2B, left panel). Still, we could detect some transcriptional upregulation of the p53 transcriptional gene target $p21^{CIP}$ (Fig. 2C). Since we failed to detect the $p21^{CIP}$ protein by western blotting in irradiated astrocytes, as opposed to irradiated NSC (Fig. S4A), this upregulation of $p21^{CIP}$ mRNA is likely insufficient to achieve a significant physiological impact. Another cell cycle controlling p53-target, GADD45α, was found unchanged, and the pro-apoptotic p53-target genes BAX and PUMA[16] were induced only very weakly (Fig. 2C). In irradiated NSC however, we detected a robust upregulation of PUMA transcript (Fig. S4B).We also tested whether DDR genes transcriptional suppression in astrocytes can be reversed by a challenge with DNA damage and performed a qRT-PCR analysis for the same DDR factors studied in Fig. 2A on irradiated astrocytes (24h after 10Gy exposure) vs unchallenged astrocytes. Remarkably, we saw no change in the DDR gene expression (Fig. 2C).

In order to test whether these findings are also applicable to adult NSC and their astrocyte descendants, we employed NSC derived from adult murine forebrain [13]**.** We derived

astrocytes from these cells and performed comparative analyses of DDR in adult NSC and astrocytes (Fig. S5). Indeed, we could observe that, upon irradiation, GFAP-expressing astrocytes have strongly attenuated phosphorylation and reduced protein levels of ATM, CHK2 and p53 when compared to parental adult NSC (Fig. S5A). Also in this setup, we found these and other DDR factors to be transcriptionally downregulated upon astrocytic differentiation (Fig. S5B).

Although we did not detect any functional activation of key DDR proteins in astrocytes, even after 50Gy of irradiation, when we performed a detailed kinetics analysis of ATM phosphorylation in irradiated astrocytes, we could detect its delayed and transient appearance by western blotting (Fig. 3A), implying a potential function for the observed residual activated ATM.

Interestingly, already 3 hours after irradiation the intensity of γH2AX signal started to diminish, 24h after irradiation γH2AX was barely detectable in astrocytes (Fig. 3A). γH2AX signal is generally considered a reliable marker of DSB presence [17]. To test whether its downregulation is the outcome of DNA damage repair or attenuation of H2AX phosphorylation in these cells, we re-irradiated astrocytes 24h after the first round of irradiation. Here, the already extinguished initial γH2AX signal could be fully detected again one hour after the second round of irradiation (Fig. 3C,D) that loss of γH2AX signal in astrocytes 24h after irradiation is not caused by an irradiation-induced decline in H2AX phosphorylation proficiency.

Noteworthy, even combined irradiation of 20Gy was unable to induce a significant increase in apoptosis as compared to not irradiated astrocytes (Fig. 3B). In NSC, already a single irradiation of 10Gy lead to distinct apoptosis when measured 72h later (Fig. 3B),

demonstrating, consistently with their lack of robust DDR signaling, that astrocytes are radioresistant as compared to parental NSC.

ATM is the main kinase involved in γH2AX generation upon DSB formation [4-5]. Yet, also the other two DNA-dependent PI3K-like protein kinases, ATR and DNA-PK, are capable of phosphorylating H2AX [17]. Our data however provide little evidence that ATR may play any functional role in astrocytes, since we could not detect ATR protein by western blotting, consistently with ATR's nature as S-phase specific PI3K-like protein kinase [17]. Differently, DNA-PKcs was expressed in astrocytes at levels comparable to NSC (Fig. 2). Based on these observations, we set on to elucidate the roles of ATM and DNA-PK in the DNA-damage induced H2AX phosphorylation in NSC and astrocytes using following small molecule inhibitors: a DNA-PK inhibitor[18] (DPKi, NU7441) and an ATM inhibitor [19] (ATMi, KU55933) or both inhibitors in combination. Under these conditions, we analyzed the intensity of γH2AX signal by two different methods: western blotting of total cell extracts (Fig. 4A) and flow cytometrical immunofluorescence analysis at the single cell level (Fig. 4B and Fig. S7). In NSC, inhibition of ATM had a profound impact on DNA damage induced phosphorylation of not only ATM-S1981, but also γH2AX as well as on the overall S/TQ phosphorylation pattern, while the inhibition of DNA-PK in NSC had no appreciable effect on any of these parameters (Fig. 4A and Fig. S6). Vice versa, in astrocytes, DNA-PK inhibitor showed a strong inhibitory impact on H2AX phosphorylation, while ATM inhibitor did not have such an effect (Fig. 4A). These findings were reproduced by flow cytometrical (Fig. 4B and Fig. S7) and immunofluorescence analyses (Fig. 4C and Fig. S8), where DNA-PK, but not ATM

inhibition in astrocytes one hour after irradiation notably reduced the population of highly γH2AX-positive cells resp. the intensity of the γH2AX signal.

We have shown ATM in astrocytes to be strongly reduced, but not to undetectable levels (Fig. 3A). Next we set on to elucidate, why its pharmacological inhibition did not lead to any reduction of γH2AX levels. We performed a COMET assay [20] under neutral conditions, which allows to directly and quantitatively detect DNA DSB in individual cells (Fig. 4D). In the COMET assay, gel electrophoresis revealed "tails" generated by broken DNA in irradiated astrocytes, and for each individual cell a so-called Olive tail moment was calculated. As above, we treated cells prior to irradiation with DPKi, ATMi or both inhibitors in combination. One hour after irradiation, the median Olive tail moment of KU55933-treated cells was significantly higher than that of DMSO or DPKi alone treated cells, indicating higher number of DSB. 24h later, cells were able to repair DNA under all conditions (as indicated by the reduction of the Olive tail moment), but significantly less efficiently when treated with both inhibitors together. These findings indicate that, despite its low expression levels, ATM plays a role in DNA repair in astrocytes and it acts in conjunction with DNA-PK. In combination with ATM inhibition, DPKi treatment lead to a significant retention of unrepaired DSB breaks in astrocytes even 24h after irradiation (Fig. 4D), indicating that ATM and DNA-PK are both involved in the DSB-repair in astrocytes.

Noteworthy, we again did not observe an apoptotic response in astrocytes three days after exposure to 10Gy irradiation, with or without additional treatments with ATMi and DNA-PKi. However, as a control, non-genotoxic cell poisons puromycin and hygromycin B were able to elicit strong apoptotic response in NSC-derived astrocytes (Fig. 4E).

NSC are also responsible for the generation of neurons. Hence, we decided to analyze the functionality of DDR signaling in NSC-derived neurons, as generated by the use of an established in vitro differentiation protocol [21]. Neurons derived in this manner stop proliferating, express markers specific for TD- neurons (such as the cytoskeletal filament protein Tuj1, also known as β-tubulin-III) and can therefore be regarded as terminally differentiated (Fig. S8A; [13]). We irradiated these neuron cultures with 10Gy in parallel with parental NSC and analyzed them under the same conditions. Tuj1 was used as a specific marker in order to detect terminally differentiated neurons by immunofluorescence and confocal microscopy (Fig. 5A). In both cell types, no nuclear pS/TQ signal was detectable in not irradiated cells (Fig. S8B). One hour after irradiation we detected formation of prominent pS/TQ foci in NSC, which stained negative for Tuj1 (Fig. 5A, upper panel). In Tuj1-positive neurons, pS/TQ foci also formed upon irradiation, their intensity being comparable to that in NSC (Fig. 5A, lower panel and Fig. S8B). We conclude that, differently from astrocytes, and consistently with previous reports [22-23], neurons do activate canonical DDR upon DNA damage, thus highlighting the unique peculiarity of astrocytes.

Finally, we extended and verified our conclusions *in vivo*. We irradiated adult mice sub-lethally with 8Gy and sacrificed them after one hour in order to study DDR activation by immunofluorescence *in vivo* in their brains (Fig. 5B). Analyses of the brain sections by confocal microscopy revealed that neurons, labeled with an antibody against the neuron-specific transcription factor NeuN, showed a diffuse nuclear 53BP1 signal, unlike adjacent GFAP-positive astrocytes (Fig. 5B, upper panel). Correspondingly, brain neurons displayed strong 53BP1 foci formation upon irradiation, while adjacent

astrocytes showed no detectable 53BP1 foci (Fig. 5B, lower panel), indicating a striking difference of DDR signaling between adjacent neurons and astrocytes *in vivo*.

Discussion

We describe here a comparative study of DDR activation and radioresistance in somatic stem cells and their terminally differentiated descendants. In our system of NSC and NSC-derived astrocytes, we have discovered that NSC show robust activation of canonical DDR signaling upon X-ray irradiation, as measured by nuclear foci assembly of activated ATM, its phosphorylation substrates pS/TQ, 53BP1 and γH2AX, and consistent DDR activation as detected by immunoblotting. This proves that NSC can mount a robust DDR activation upon genotoxic stress and highlights the different regulation of DDR in these somatic stem cells and the embryonic stem cells (from which our NSC derive), which have been reported to show reduced checkpoints and dysfunctional DDR protein localization and functions [24].

Surprisingly however, we observed, both *in vitro* and *in vivo*, that the activation of ATM and its downstream DDR factors were strongly inhibited in astrocytes. We show that the mechanism of DDR inhibition involves a stable transcriptional repression of key DDR genes. The astrocytes used in our study are non-proliferating terminally differentiated cells, thus reproducing the state of the overwhelming majority of adult brain astrocytes [25]. Deficits in this key feature are the likely reason for a certain degree of DDR activation observed in proliferating astrocytic lines [26-27] and differentiated astrocytes displaying residual proliferation [28]. Importantly, downregulation of DDR is peculiar of astrocytes and is not necessarily associated with terminal differentiation. Indeed, as a relevant

comparison, we show that neurons display a detectable DDR both *in vitro* and *in vivo*. Similar conclusions in regard to ATM activation in neurons have been reported [22].

At the current stage, one can speculate if the evolutionary reason for astrocytes to downregulate DDR signaling is to avoid apoptosis upon genotoxic stress. We show that TD astrocytes are, unlike the parental NSC, radioresistant and do not undergo apoptosis upon irradiation. Similar observations were made in TD muscle cells, where the DDR cascade was suppressed at the p53 level [29]. Irradiation-induced tissue failures may hence derive from the demise of respective stem and progenitor cells, and not TD cells. As we show here, the apoptosis-controlling ATM-CHK2-p53[20] axis in astrocytes is strongly attenuated by the transcriptional downregulation of these genes. Indeed, the pro-apoptotic p53 target gene PUMA is hardly induced in irradiated astrocytes, consistent with the observed lack of apoptosis. In NSC, we detected a clear apoptotic response and PUMA was found strongly upregulated, confirming the role of this p53-target in stem cell apoptosis [30]. In neurons, p53-dependent cell death upon genotoxic stress was also reported, and sometimes associated with their re-entry into cell cycle [31-32], while *in vivo* astrocytes are only known to re-enter cell cycle under pathological condition of reactive gliosis [25]. In this respect in would be interesting to check whether DDR and apoptosis proficiency of brain astrocytes increases when they undergo injury-induced reactive gliosis. It is therefore possible that different TD cell types are differently radiosensitive, depending on their specific role and physiological context.

Despite suppressed DDR signaling pathways, DNA damaged-induced phosphorylation of H2AX at S139 is still clearly detectable in astrocytes. γH2AX formation upon DNA damage is commonly associated with ATM function, yet ATM is downregulated and its

residual activation is very much delayed compared with the rapid and efficient γH2AX foci assembly in these cells. ATR expression is inhibited too; this is expected given its specialized role in DNA replication [17]. The third family member of the DNA dependent PI3K-like kinases, DNA-PK, is a key enzyme in DSB repair. The DNA-PK-dependent NHEJ repair pathway is the main DSB repair pathway used in non-proliferating cells. We found DNA-PK and other key NHEJ genes to be expressed in differentiated astrocytes. Moreover, we revealed that in TD-astrocytes, DNA-PK is actually responsible for DNA damage induced H2AX phosphorylation, unlike in NSC, where ATM appears to be the main responsible kinase. Such substituting role of DNA-PK in cells lacking robust ATM activity is consistent with observations in ATM-deficient cells [33-35] and mouse models [36-37], in which DNA-PK can take over the role of ATM in phosphorylating H2AX. It is worth considering that ATM cannot be directly recruited to DSB, rather requiring the DNA-binding role of proteins of the MRE11/RAD50/NBS1 complex [1], which we found strongly downregulated in astrocytes. Yet DNA-PKcs is recruited to broken DNA ends through its KU70/80 subunits [38]. This binding to DSB would enable the DNA-PK complex to exert its kinase activity on proximal H2AX despite the transcriptionally suppressed apical DDR signaling cascade in astrocytes.

The disappearance of γH2AX foci in astrocytes can be interpreted as successful DNA repair and indeed, DSB repair is functional in these cells, as demonstrated by COMET assays. However we observed that in astrocytes inhibition of DNA-PK alone is not sufficient to significantly impair DNA repair in irradiated astrocytes, unless combined with inhibition of ATM. We could indeed detect some amount of delayed ATM activity in irradiated astrocytes. Apparently, these marginal levels of ATM in astrocytes are

responsible for DNA repair. This may be a valuable observation when considering Ataxia-telangiectasia patients carrying reduced but not completely absent ATM activity or mouse models with hypomorphic ATM alleles.

It remains to be elucidated which mechanisms might be responsible for downregulation of DDR in astrocytes and maybe other TD cells, and for the qualitative differences in DDR proficiency among various types of TD cells. DSB repair kinetics are not equal among cell types [39] and we have preliminary evidence that in NSC it is faster than in TD astrocytes (data not shown). But also among similar tissues, the efficiency of γH2AX foci formation and DNA repair vary in age-related manner in TD cells [40]. Further research also is needed to uncover the physiological and evolutionary reasons on the diversity of DDR, DNA-repair pathways and radioresistance in somatic stem cells and various kinds of terminally differentiated cells in developing and adult organisms.

Materials and Methods

Cell culture and treatments

Murine ES-derived neural stem cells (NSC, [13]) were grown in Euromed-N cell culture medium (Euroclone), supplemented with 2mM L-glutamine, 100U/ml penicillin and 100µg/ml streptomycin, 1x N2 supplement (Invitrogen), 20ng/ml murine EGF and FGF2 (ProSpec, Israel) at 5% CO2 and 37° C. Astrocyte differentiation and culture medium was DMEM/F12 with 2mM L-glutamine, 100U/ml penicillin, 100µg/ml streptomycin and 10% FCS. Neuron differentiation was performed as described in [21]. NU7441[18] and KU55933[19] (Tocris) were dissolved in DMSO and used at 1µM final concentration overnight prior to irradiation. X-ray irradiation of cells was performed in a Faxitron RX-650 device for 5 min at 2Gy/min (total of 10Gy).

Immunoblotting

Cells were lysed in NP40 lysis buffer (1% NP40, 50mM Tris-Cl pH 8, 150mM NaCl, 2mM EDTA, 1mM DTT, 1mM NaF, 100µM Na_2VO_4 and protease inhibitor cocktail (Roche) or in Lämmli lysis buffer (for γH2AX analysis) and 20-50µg of whole cell lysate in Lämmli loading buffer were resolved by SDS-PAGE, transferred to nitrocellulose membranes (Protran) using Biorad electrophoresis systems and probed with primary and secondary antibodies in 5% bovine serum albumin (BSA) and skimmed milk, respectively.

Antibodies

Mouse monoclonal antibodies against: Nestin, CHK2, γH2AX (Millipore); ATM, vinculin, α-tubulin (Sigma Aldrich); ATM pS1981* (Rockland); Nestin (BD Biosciences); Tuj1 (Covance); NeuN (Abcam). Rabbit poly- and monoclonal antibodies

against: GFAP (Dako); pS/TQ, p53 pS15 (Cell Signaling Technology); p53 (FL393) (Santa Cruz Biotechnologies); 53BP1 (Novus); Chicken polyclonal antibody against GFAP (Abcam). *S1981 of human ATM, against which the antibody was generated, corresponds to Ser1987 of the murine ATM (Pellegrini et al, *Nature*, 2006).

Immunofluorescence microscopy

Cells cultured on glass cover slips were fixed in methanol/acetone (1:1, 3 minutes at room temperature), blocked with 0.5% BSA and 0.2% gelatin in PBS, thenprobed with appropriate primary antibodies and Alexa-fluor 488-, 568- and 647-labeled secondary antibodies (Invitrogen). DNA was counterstained with DAPI (Sigma Aldrich). Confocal images were obtained with a Leica TCS SP2 AOBS confocal laser microscope by sequential scanning.

Gene expression analysis

Total RNA was extracted from live cells with Trizol reagent (Invitrogen), precipitated with isopropanol and ethanol and dissolved in DEPC-treated water (Invitrogen). 1 µg of total RNA (as quantified with NanoVue device, General Electric (GE)) was used for retrotranscription using VILO reverse transcription kit (Invitrogen) according to manufacturer's instructions and without RNAse treatment. RT- reactions (without reverse transcriptase enzyme) were prepared. Estimated 20ng of cDNA in 25µl reaction volume were analyzed in triplicate by quantitative RT-PCR amplification on a Light Cycler 480 system (Roche) using SYBR Green assay (QuantiFast SYBR Green PCR Kit, Qiagen) according to manufacturer's instructions and for 40 cycles. CT-values were obtained by calculation of the second derivative using Light Cycler 480 software (Roche) and normalized among samples against the housekeeping gene (B2M). RT- preparations on

the housekeeping gene proved to be negative. Forward and reverse primers (FP and RP) were designed with Roche UniversalProbe Library software against *Mus musculus*:

B2M: FP: CTGCAGAGTTAAGCATGCCAGTA; RP: TCACATGTCTCGATCCCAGTAGA

ATM: FP: TGCAGATTTATATCCATCATCCAC; RP: TTTCATGGATTCATAAGCACCTT

53BP1: FP: AAAGTCTGCCACCGTGAAAC; RP: TCTCCAGTCTCACAGGGACTC

MRE11: FP: CTTTTTCAGGCACAGGGAAC; RP: TGTGATGAGCATCCCAAAGT

MDC1: FP: AGGGCAGCTACGTCTCTTCA; RP: CCAAGGTAGAGGGGGAAATC

CHK2: FP: TTATTCCTGAAGTCTGGACAGATG; RP: CTAACAGTTTCTTGACAAGGTCCA

p53: FP: ACGCTTCTCCGAAGACTGG; RP: AGGGAGCTCGAGGCTGATA

DNA-PKcs: FP: TGCAGAGAAATGTGATTGCAC; RP: CCACGGTGGAAGATCTTTTG

KU70: FP: CAGAACATTCAGGTGACTCCAG; RP: GCACCTTCCGCTTGTCAT

KU80: FP: GAAGATCACATCAGCATCTCCA; RP: CAGGATTCACACTTCCAACCT

XRCC4: FP: TGCATAAATTGCTAAATGAAGTCC; RP: TTGTCAGAACACGGATTTTCC

LIG4: 5': GAAGAAATCGTGTCCTGATGC; RP: CAAATCCTCCGGTTTGAACT

Flow cytometry:

For γH2AX assay, cells were fixed in 75% ethanol (1h, 4°C),) washed with 1% BSA in PBS and stained with mouse-anti-γH2AX antibody (Millipore), followed by Alexa-fluor-488 labeled secondary antibody (Invitrogen). For TUNEL assay, cells were fixed in 2% paraformaldehyde (PFA, 20 minutes at 4°C) permeabilized in 75% ethanol, washed with 1% BSA in PBS and treated with "In Situ Cell Death Detection Kit, Fluorescein" (Roche), followed by staining with propidium iodide (Sigma Aldrich). FACS acquisition and analysis were performed on BD FACScalibur using CellQuest software.

COMET assay

Assay was performed with CometSlide kit (Trevigen) according to manufacturer's instructions for neutral electrophoresis. Between 100 and 200 cells we scored for each

experimental condition. COMET tails were analyzed with CometScore 1.5 software, statistical significance of Olive tail moment medians was calculated using Dunn's Method for multiple comparisons versus control group.

In vivo DNA damage assays

Adult mice of C57BL6 strain of 10-12 weeks of age were irradiated with 8 Gy (using a GammaCell 220 device (Nordion) with ^{60}Cobalt as radiation source at about 0.25 Gy/s) and sacrificed 6h after irradiation. Brains were cryopreserved in optimal cutting temperature (O.C.T.) compound (Tissue-Tek). Longitudinal 10 micron thick sections were fixed in 3.7% formaldehyde, permeabilized with 0.5% Triton X100, blocked with 5% goat serum and incubated overnight at 4°C with primary antibodies, followed by incubation at room temperature with AlexaFluor 488, 568 or 647labeled secondary antibodies. Cell nuclei were counterstained with DAPI (Sigma Aldrich). Confocal microscopy was performed as above.

Acknowledgements

We thank Luciano Conti and Elena Cattaneo for advice, discussions and sharing of protocols and reagents, Thomas Burgold and Giuseppe Testa for help with the establishing of NSC cultures, Barbara Giulini and Alberto Gobbi for help with experimental animal handling, Sara Tomassini for experimental help and all F.d'A.d.F. lab members for discussion and feedback throughout this work.

Conflict of interest:

We declare that there are no conflicts of interests.

References

1. Shiloh Y. The ATM-mediated DNA-damage response: taking shape. *Trends in Biochemical Sciences* 2006; **31**(7)**:** 402-410.

2. d'Adda di Fagagna F. Living on a break: cellular senescence as a DNA-damage response. *Nat Rev Cancer* 2008; **8**(7)**:** 512-22.

3. Freeman MR. Specification and Morphogenesis of Astrocytes. *Science* 2010; **330**(6005)**:** 774-778.

4. Bakkenist CJ, Kastan MB. DNA damage activates ATM through intermolecular autophosphorylation and dimer dissociation. *Nature* 2003; **421**(6922)**:** 499-506.

5. Burma S, Chen BP, Murphy M, Kurimasa A, Chen DJ. ATM Phosphorylates Histone H2AX in Response to DNA Double-strand Breaks. *Journal of Biological Chemistry* 2001; **276**(45)**:** 42462-42467.

6. Schultz LB, Chehab NH, Malikzay A, Halazonetis TD. P53 Binding Protein 1 (53bp1) Is an Early Participant in the Cellular Response to DNA Double-Strand Breaks. *The Journal of cell biology* 2000; **151**(7)**:** 1381-1390.

7. Jowsey P, Morrice NA, Hastie CJ, McLauchlan H, Toth R, Rouse J. Characterisation of the sites of DNA damage-induced 53BP1 phosphorylation catalysed by ATM and ATR. *DNA Repair* 2007; **6**(10)**:** 1536-1544.

8. Khanna KK, Jackson SP. DNA double-strand breaks: signaling, repair and the cancer connection. *Nature genetics* 2001; **27**(3)**:** 247-254.

9. Mahaney BL, Meek K, Lees-miller SP. Repair of ionizing radiation-induced DNA double-strand breaks by non-homologous end-joining. *Biochem J* 2009; **417**(3)**:** 639-650.

10. Doetsch F. The glial identity of neural stem cells. *Nat Neurosci* 2003; **6**(11)**:** 1127-1134.

11. Schull WJ. Brain damage among individuals exposed prenatally to ionizing radiation: A 1993 review. *Stem Cells* 1997; **15**(S1)**:** 129-133.

12. Kal HB, Struikmans H. Radiotherapy during pregnancy: fact and fiction. *The Lancet Oncology* 2005; **6**(5)**:** 328-333.

13. Conti L, Pollard SM, Gorba T, Reitano E, Toselli M, Biella G *et al.* Niche-independent symmetrical self-renewal of a mammalian tissue stem cell. *PLoS biology* 2005; **3**(9)**:** e283.

14. Noon AT, Shibata A, Rief N, Lobrich M, Stewart GS, Jeggo PA *et al.* 53BP1-dependent robust localized KAP-1 phosphorylation is essential for heterochromatic DNA double-strand break repair. *Nature cell biology* 2010; **12**(2)**:** 177-184.

15. Canman CE, Lim D-S, Cimprich KA, Taya Y, Tamai K, Sakaguchi K *et al.* Activation of the ATM Kinase by Ionizing Radiation and Phosphorylation of p53. *Science* 1998; **281**(5383)**:** 1677-1679.

16. Roos WP, Kaina B. DNA damage-induced cell death by apoptosis. *Trends in molecular medicine* 2006; **12**(9)**:** 440-50.

17. Kinner A, Wu W, Staudt C, Iliakis G. γ-H2AX in recognition and signaling of DNA double-strand breaks in the context of chromatin. *Nucleic acids research* 2008; **36**(17)**:** 5678-5694.

18. Leahy JJJ, Golding BT, Griffin RJ, Hardcastle IR, Richardson C, Rigoreau L *et al.* Identification of a highly potent and selective DNA-dependent protein kinase (DNA-PK) inhibitor (NU7441) by screening of chromenone libraries. *Bioorganic & Medicinal Chemistry Letters* 2004; **14**(24)**:** 6083-6087.

19. Hickson I, Zhao Y, Richardson CJ, Green SJ, Martin NMB, Orr AI *et al.* Identification and Characterization of a Novel and Specific Inhibitor of the Ataxia-Telangiectasia Mutated Kinase ATM. *Cancer research* 2004; **64**(24)**:** 9152-9159.

20. Olive PL. Impact of the comet assay in radiobiology. *Mutation Research/Reviews in Mutation Research* 2007; **681**(1)**:** 13-23.

21. Spiliotopoulos D, Goffredo D, Conti L, Di Febo F, Biella G, Toselli M *et al.* An optimized experimental strategy for efficient conversion of embryonic stem (ES)-derived mouse neural stem (NS) cells into a nearly homogeneous mature neuronal population. *Neurobiology of Disease* 2009; **34**(2)**:** 320-331.

22. Biton S, Gropp M, Itsykson P, Pereg Y, Mittelman L, Johe K *et al.* ATM-mediated response to DNA double strand breaks in human neurons derived from stem cells. *DNA Repair* 2007; **6**(1)**:** 128-134.

23. Gorodetsky E, Calkins S, Ahn J, Brooks PJ. ATM, the Mre11/Rad50/Nbs1 complex, and topoisomerase I are concentrated in the nucleus of Purkinje neurons in the juvenile human brain. *DNA Repair* 2007; **6**(11)**:** 1698-1707.

24. Hong Y, Cervantes RB, Tichy E, Tischfield JA, Stambrook PJ. Protecting genomic integrity in somatic cells and embryonic stem cells. *Mutation research* 2007; **614**(1-2)**:** 48-55.

25. Buffo A, Rolando C, Ceruti S. Astrocytes in the damaged brain: Molecular and cellular insights into their reactive response and healing potential. *Biochemical Pharmacology* 2010; **79**(2)**:** 77-89.

26. Bartkova J, Hamerlik P, Stockhausen MT, Ehrmann J, Hlobilkova A, Laursen H *et al.* Replication stress and oxidative damage contribute to aberrant constitutive activation of DNA damage signalling in human gliomas. *Oncogene* 2010; **29**(36)**:** 5095-5102.

27. Burdak-Rothkamm S, Short SC, Folkard M, Rothkamm K, Prise KM. ATR-dependent radiation-induced [gamma]H2AX foci in bystander primary human astrocytes and glioma cells. *Oncogene* 2006; **26**(7)**:** 993-1002.

28. Adams BR, Golding SE, Rao RR, Valerie K. Dynamic Dependence on ATR and ATM for Double-Strand Break Repair in Human Embryonic Stem Cells and Neural Descendants. *PLoS ONE* 2010; **5**(4)**:** e10001.

29. Latella L, Lukas J, Simone C, Puri PL, Bartek J. Differentiation-Induced Radioresistance in Muscle Cells. *Molecular and Cellular Biology* 2004; **24**(14)**:** 6350-6361.

30. Akhtar RS, Geng Y, Klocke BJ, Latham CB, Villunger A, Michalak EM *et al.* BH3-Only Proapoptotic Bcl-2 Family Members Noxa and Puma Mediate Neural Precursor Cell Death. *Journal of Neuroscience* 2006; **26**(27)**:** 7257-7264.

31. Morrison RS, Kinoshita Y, Johnson MD, Guo W, Garden GA. p53-Dependent Cell Death Signaling in Neurons. *Neurochemical Research* 2003; **28**(1)**:** 15-27.

32. Barzilai A, Biton S, Shiloh Y. The role of the DNA damage response in neuronal development, organization and maintenance. *DNA Repair* 2008; **7**(7)**:** 1010-1027.

33. Takahashi A, Mori E, Su X, Nakagawa Y, Okamoto N, Uemura H *et al.* ATM is the Predominant Kinase Involved in the Phosphorylation of Histone H2AX after Heating. *Journal of Radiation Research* 2010; **51**(4)**:** 417-422.

34. Stiff T, O'Driscoll M, Rief N, Iwabuchi K, Löbrich M, Jeggo PA. ATM and DNA-PK Function Redundantly to Phosphorylate H2AX after Exposure to Ionizing Radiation. *Cancer research* 2004; **64**(7)**:** 2390-2396.

35. Reitsema T, Klokov D, Banáth JP, Olive PL. DNA-PK is responsible for enhanced phosphorylation of histone H2AX under hypertonic conditions. *DNA Repair* 2005; **4**(10)**:** 1172-1181.

36. Koike M, Sugasawa J, Yasuda M, Koike A. Tissue-specific DNA-PK-dependent H2AX phosphorylation and [gamma]-H2AX elimination after X-irradiation in vivo. *Biochemical and biophysical research communications* 2008; **376**(1)**:** 52-55.

37. Bellani MA, Romanienko PJ, Cairatti DA, Camerini-Otero RD. SPO11 is required for sex-body formation, and Spo11 heterozygosity rescues the prophase arrest of Atm-/- spermatocytes. *Journal of Cell Science* 2005; **118**(15)**:** 3233-3245.

38. Yano K-i, Morotomi-Yano K, Adachi N, Akiyama H. Molecular Mechanism of Protein Assembly on DNA Double-strand Breaks in the Non-homologous End-joining Pathway. *Journal of Radiation Research* 2009; **50**(2)**:** 97-108.

39. Hande MP, Natarajan AT. Induction and Persistence of Cytogenetic Damage in Mouse Splenocytes Following Whole-Body X-Irradiation Analysed by Fluorescence In Situ Hybridisation. V. Heterogeneity/Chromosome Specificity. In: Nakashima M, Takamura N, Tsukasaki K, Nagayama Y, Yamashita S (eds). *Radiation Health Risk Sciences*. Springer Japan, 2009, pp 143-149.

40. Hudson D, Kovalchuk I, Koturbash I, Kolb B, Martin OA, Kovalchuk O. Induction and persistence of radiation-induced DNA damage is more pronounced in young animals than in old animals. *Aging (Albany NY)* 2011.

Figure Legends

Fig. 1. NSC show efficient DDR activation while this is strongly impaired in NSC-derived astrocytes

A One hour after irradiation with 10Gy, NSC (here, negative for intermediate filament GFAP) uniformly display ATM kinase activity as demonstrated by the detection of foci of autophosphorylated ATM (S1981), ATM/ATR/DNA-PK specific phospho-epitopes (pS/TQ), 53BP1 and of the phosphorylated histone H2AX (γH2AX), as analysed by confocal microscopy of immunofluorescence stainings. Bar: 15μm.

B In contrast, astrocytes (positive for intermediate filament GFAP) when irradiated and treated in parallel with NSC, show only marginal phospho-ATM foci appearance and nearly no nuclear signal of 53BP1 or pS/TQ foci. However, astrocytes still display irradiation-induced nuclear γH2AX signal. Bar: 15μm

Fig. 2. DDR response factors are transcriptionally suppressed in astrocytes, while NSC show canonical DDR upon irradiation.

A Quantitative RT-PCR analysis reveals a transcriptional downregulation of DDR genes, but retained expression of DNA repair factors, in astrocytes. Expression profiles were normalized against parental NSC prior to serum-induced differentiation. β2-microglobulin was used as housekeeping gene.

B Western blot analysis of NSC and astrocytes, irradiated and processed in parallel. Membranes were probed with phospho-specific and total antibodies as shown and normalized for vinculin.

C Quantitative RT-PCR analysis showing that even 24h following irradiation, key DDR factors remain downregulated in astrocytes. Four target genes of p53 were also analysed: transcripts of GADD45a, BAX and PUMA remained largely unchanged. The mRNA of the cell cycle control gene $p21^{CIP}$ was found upregulated. Expression profiles were normalized against not irradiated astrocytes. β2-microglobulin was used as housekeeping gene.

Fig. 3. Residual ATM activity can be detected in irradiated astrocytes and parallels the downregulation of the γH2AX signal.

A Western blot analysis of DDR kinetics in astrocytes, irradiated with 10Gy. Weak and transient phospho-ATM signal can be detected and coincides with reduction of γH2AX and increase in p53 signal. Note that even 50Gy fail to induce any strong DDR in astrocytes. Irradiated NSC were used as positive control. Membranes were probed with phospho-specific and total antibodies and normalized for vinculin.

B TUNEL assay for apoptosis-induced DSB in astrocytes 72h after irradiation with 10Gy. Note that also re-irradiation with further 10Gy 24h after the first exposure to X-rays fails to induce apoptosis. NSC 72h after 10Gy irradiation show a profound induction of apoptosis compared to not irradiated NSC.

C Immunofluorescence analysis showing the DNA-damage induced appearance of γH2AX signal in irradiated astrocytes. 24h later, the foci are strongly downregulated, indicating repair. Another round of irradiation leads to a de novo

formation of the γH2AX signal, indicating a still functional H2AX phosphorylation machinery. Bar: ~22μm.

D Similar observations can also be made by western blot analysis. Membrane was probed with phospho-specific and total antibody against H2AX and normalized for α-tubulin.

Fig. 4. Astrocytes display functional ATM-biased DNA repair and DNA-PK biased H2AX phosphorylation, but no apoptotic response upon irradiation.

A Western blot analysis of NSC and astrocytes, treated with solvent (DMSO) or DNA-PK inhibitor NU7441 and ATM inhibitor KU55933, separately or in combination (NU+KU) at concentrations of 1 μM each (lower than IC50 values of the inhibitor's second most sensitive PI3K-like protein kinase target), irradiated and processed in parallel. The membrane was probed for phosphorylated and total form of H2AX and normalized with vinculin.

B Flow cytometrical analysis of astrocytes, treated with inhibitors as above, irradiated and stained with antibody against γH2AX. Alexa488 secondary antibody signal was measured on $\log_{10}$ scale. Gates were set to discriminate γH2AX-negative cells, while γH2AX positive cells were arbitrarily subdivided into high and low positive. Same gateset was used for all measurements of each experiment done in quadruplicate. Error bars show SD.

C Confocal immunofluorescence analysis of astrocytes irradiated with 1Gy to better discriminate γH2AX foci. Note the reduction of the γH2AX signal intensity in irradiated astrocytes, treated with DNA-PK inhibitor NU7441. Bar: 10μm.

D DSB detection by neutral COMET assay in astrocytes 1h and 24h after irradiation, treated with inhibitors as above. Olive tail moments are presented as box plot diagram, with vertical bars indicating median values. Error bars show standard deviation (SD). Significance of the median values was calculated with Dunn's method with DMSO treated cells as control group. ‡ same significance ratio applies when not irradiated cells are used as reference.

E TUNEL assay for apoptosis-induced DSB in astrocytes 24h and 72h after irradiation, treated with inhibitors as above. As positive control for apoptotic proficiency of astrocytes, cells were treated for 2 days with puromycin (5μg/ml) or hygromycin (800μg/ml).

Fig. 5. NSC- derived neurons are DDR-proficient. Also *in vivo* neurons show robust DDR upon irradiation, as opposed to brain astrocytes.

A Terminally differentiated neurons were derived from NSC according to an established differentiation protocol [21]. One hour after irradiation with 10Gy both NSC (here, negative for neuronal marker Tuj1) and NSC-derived neurons (Tuj1 positive) show robust ATM kinase activity through appearance of foci of phospho-epitope (pS/TQ) as analysed by confocal immunofluorescence. Bar: 10μm.

B Wild-type mice were untreated or irradiated with a sub-lethal dose of 8Gy and sacrificed for brain analysis after 6 hours. Neurons were detected using nuclear neuron marker NeuN and astrocytes using intermediate filament GFAP. Activation of DDR was assessed through formation of 53BP1 foci upon

irradiation. Neurons show 53BP1 foci assembly 6h after 8Gy delivery, while astrocytes do not. Note that astrocytes also lack the diffuse nuclear 53BP1 signal present in neurons. Bar: 10μm. Note: GFAP protein in brain astrocytes is known to localize only in their cellular protrusions, hence different signal appearance from GFAP of *in vitro* astrocytes.

Fig 1

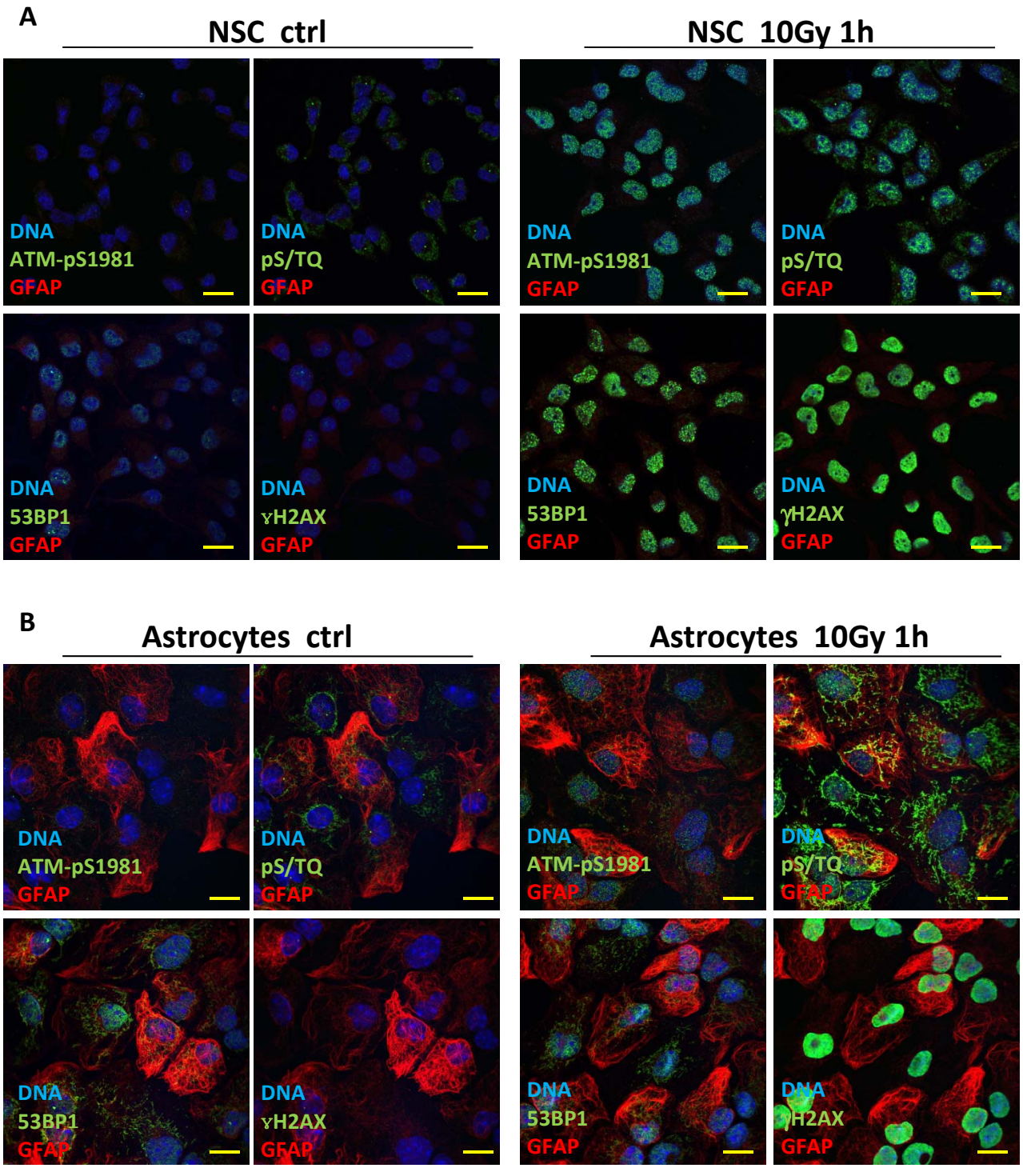
A
NSC ctrl
NSC 10Gy 1h
DNA
ATM-pS1981
GFAP
DNA
pS/TQ
GFAP
DNA
53BP1
GFAP
DNA
γH2AX
GFAP
B
Astrocytes ctrl
Astrocytes 10Gy 1h

Fig 2

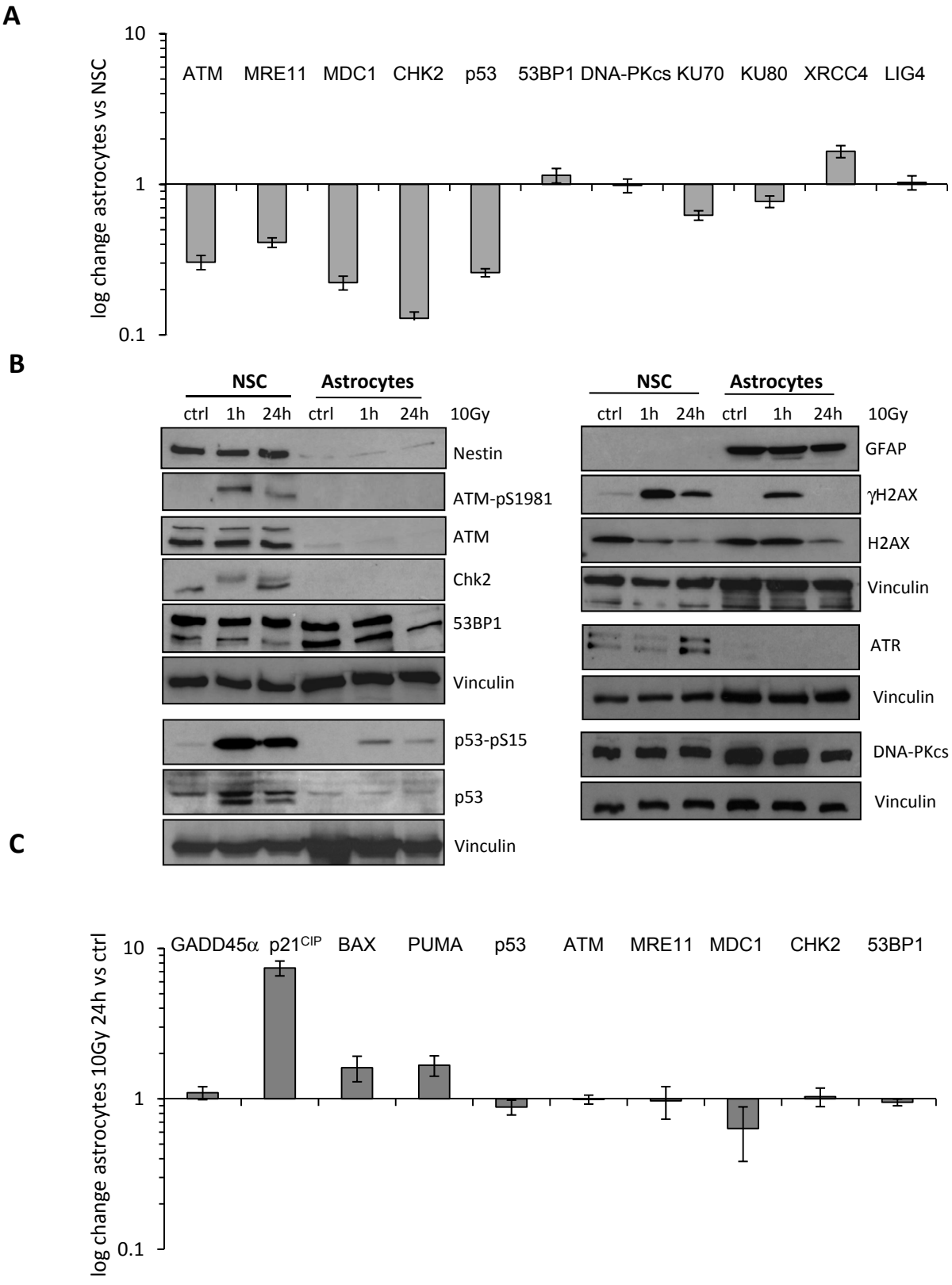
A
10
1
0.1
log change astrocytes vs NSC
ATM
MRE11
MDC1
CHK2
p53
53BP1
DNA-PKcs
KU70
KU80
XRCC4
LIG4
B
NSC
Astrocytes
ctrl
1h
24h
ctrl
1h
24h
10Gy
Nestin
ATM-pS1981
ATM
Chk2
53BP1
Vinculin
p53-pS15
p53
Vinculin
NSC
Astrocytes
ctrl
1h
24h
ctrl
1h
24h
10Gy
GFAP
γH2AX
H2AX
Vinculin
ATR
Vinculin
DNA-PKcs
Vinculin
C
10
1
0.1
log change astrocytes 10Gy 24h vs ctrl
GADD45α
p21CIP
BAX
PUMA
p53
ATM
MRE11
MDC1
CHK2
53BP1

Fig 3

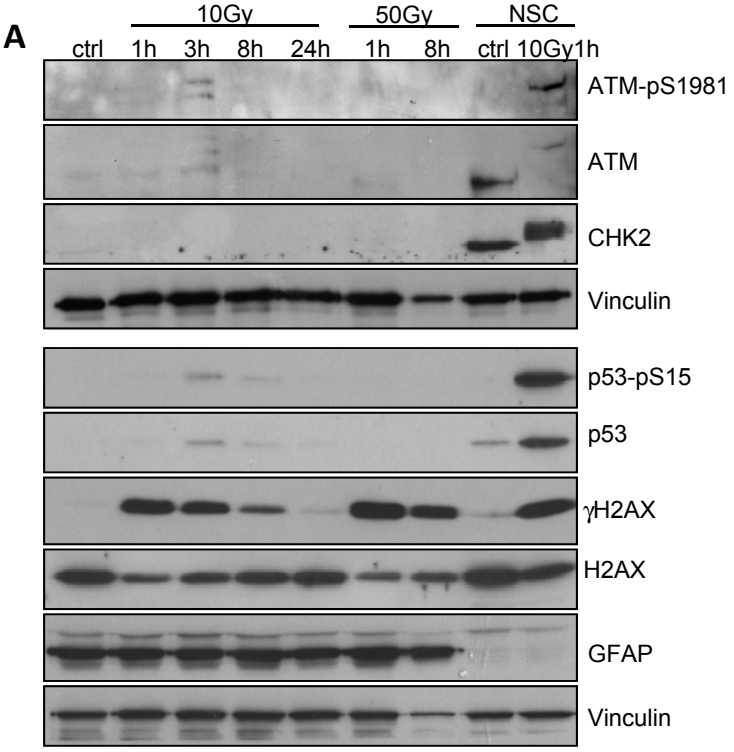
A
10Gy
50Gy
NSC
ctrl 1h 3h 8h 24h 1h 8h ctrl 10Gy1h
ATM-pS1981
ATM
CHK2
Vinculin
p53-pS15
p53
γH2AX
H2AX
GFAP
Vinculin

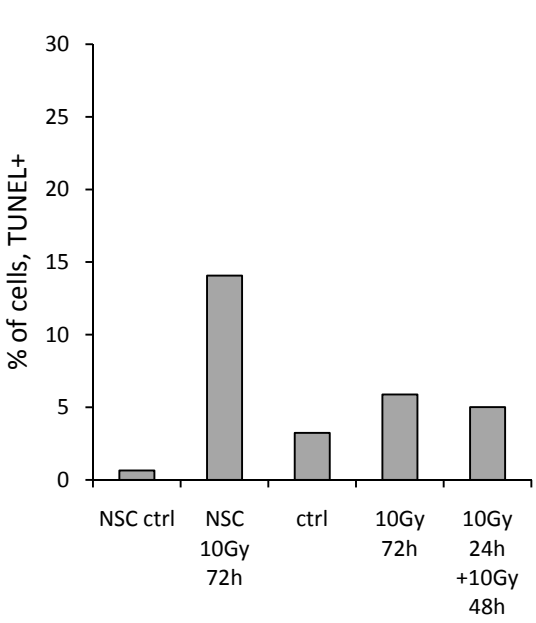
B
% of cells, TUNEL+
30
25
20
15
10
5
0
NSC ctrl
NSC 10Gy 72h
ctrl
10Gy 72h
10Gy 24h +10Gy 48h

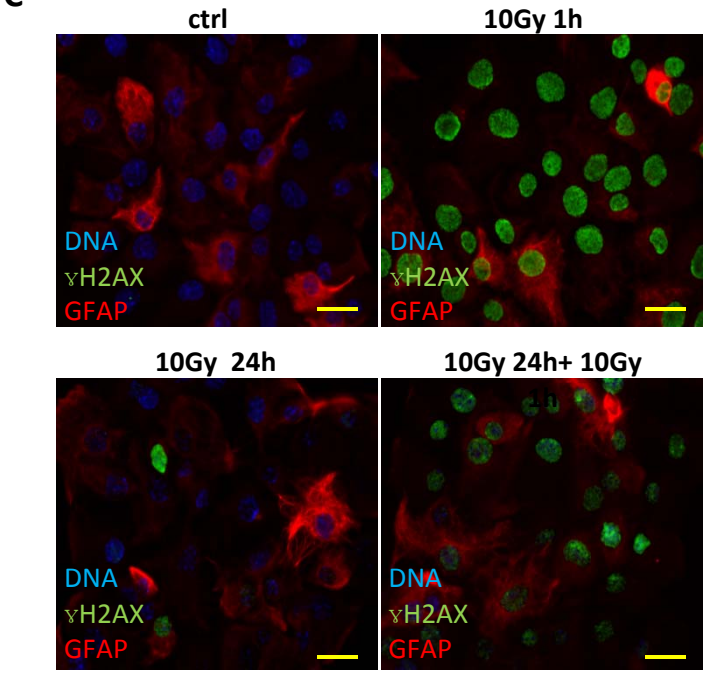
C
ctrl
10Gy 1h
10Gy 24h
10Gy 24h+ 10Gy
DNA
γH2AX
GFAP

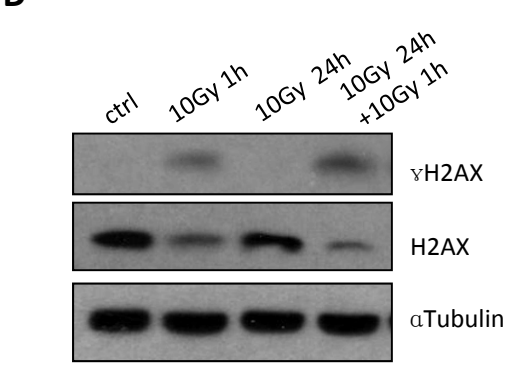
D
ctrl
10Gy 1h
10Gy 24h
10Gy 24h +10Gy 1h
γH2AX
H2AX
αTubulin

Fig 4

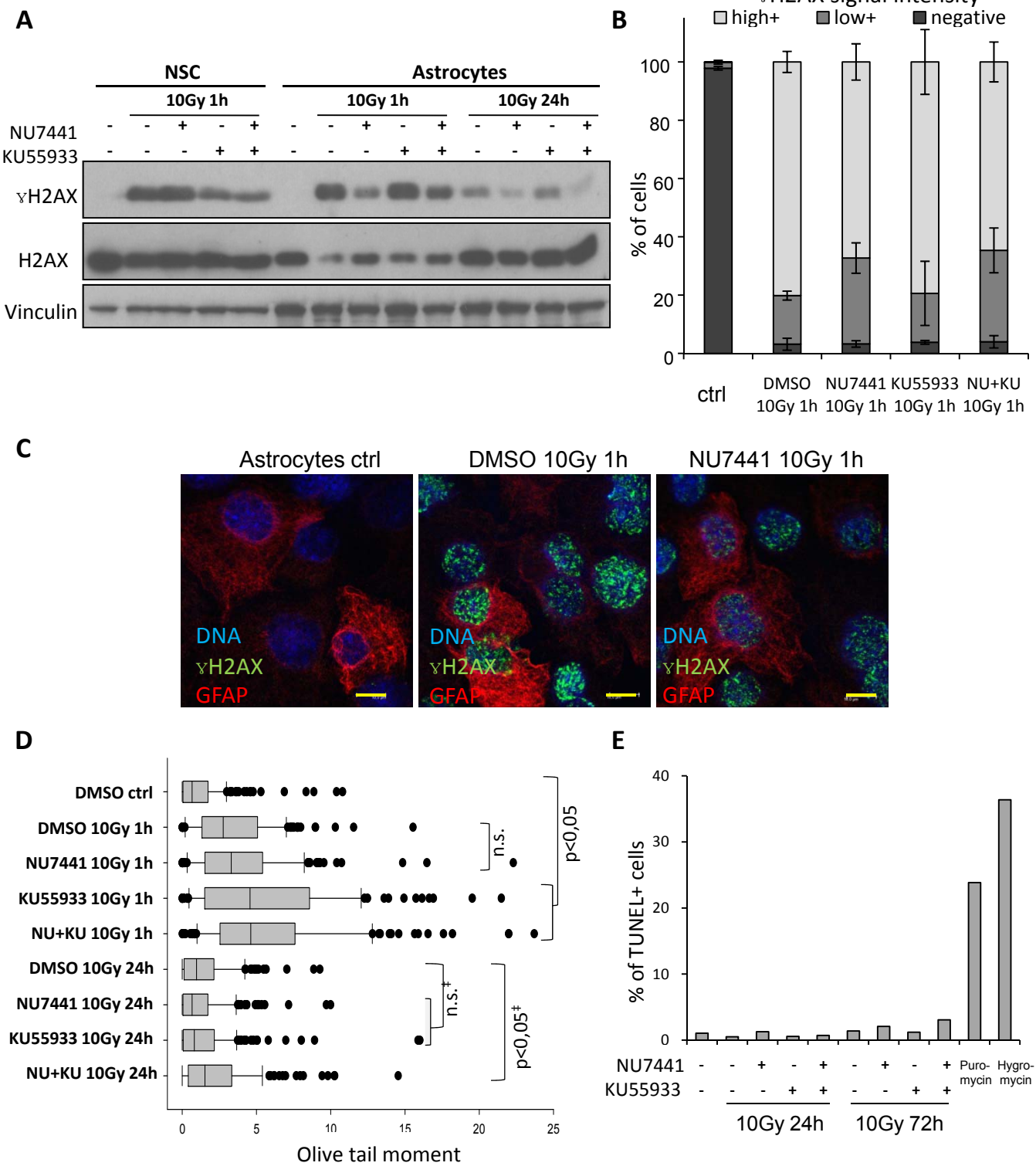
A
NSC
Astrocytes
10Gy 1h
10Gy 1h
10Gy 24h
NU7441
KU55933
γH2AX
H2AX
Vinculin
B
γH2AX signal intensity
high+
low+
negative
% of cells
ctrl
DMSO 10Gy 1h
NU7441 10Gy 1h
KU55933 10Gy 1h
NU+KU 10Gy 1h
C
Astrocytes ctrl
DMSO 10Gy 1h
NU7441 10Gy 1h
DNA
γH2AX
GFAP
D
DMSO ctrl
DMSO 10Gy 1h
NU7441 10Gy 1h
KU55933 10Gy 1h
NU+KU 10Gy 1h
DMSO 10Gy 24h
NU7441 10Gy 24h
KU55933 10Gy 24h
NU+KU 10Gy 24h
n.s.
p<0,05
n.s.
p<0,05‡
Olive tail moment
E
% of TUNEL+ cells
NU7441
KU55933
Puro-mycin
Hygro-mycin
10Gy 24h
10Gy 72h

Fig 5

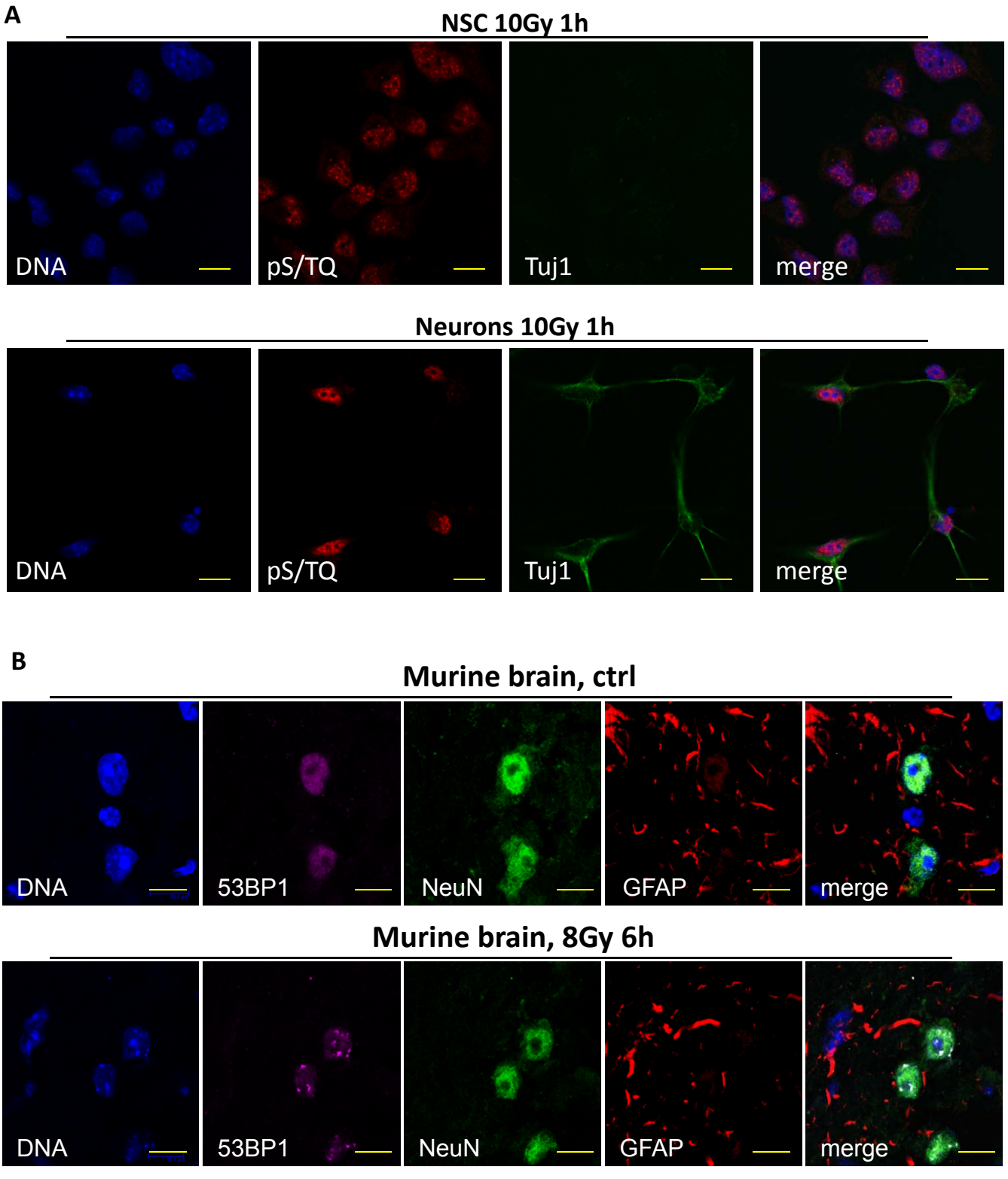
A
NSC 10Gy 1h
DNA
pS/TQ
Tuj1
merge
Neurons 10Gy 1h
DNA
pS/TQ
Tuj1
merge
B
Murine brain, ctrl
DNA
53BP1
NeuN
GFAP
merge
Murine brain, 8Gy 6h
DNA
53BP1
NeuN
GFAP
merge